ACS APPLIED MATERIALS & INTERFACES

Research Article

www.acsami.org

In vitro Investigation on the Biodegradability and Biocompatibility of Genipin Cross-linked Porcine Acellular Dermal Matrix with Intrinsic Fluorescence

Jichuan Qiu,[†] Jianhua Li,[†] Guancong Wang,[‡] Lin Zheng,[§] Na Ren,[†] Hong Liu,*[,†] Wei Tang,[§] Huaidong Jiang,[†] and Yingjun Wang*[,∥]

[†]Bio-Micro-Nano Functional Materials Center, State Key Laboratory of Crystal Materials, Shandong University, Jinan, 250100, China

[‡]The Centre for Research and Technology Development, Shandong Energy Group Co., Ltd., Jinan, 250014, China

[§]School of Medicine, Shandong University, Jinan 250012, China

[∥]National Engineering Research Center for Tissue Restoration and Reconstruction, South China University of Technology, Guangzhou, 510640, China

Supporting Information

ABSTRACT: As a biocompatible and bioactive natural tissue engineering scaffold, porcine acellular dermal matrix (PADM) has limitations for the application in tissue regeneration due to its low strength and rapid biodegradation. Here, purified PADM was modified by a nontoxic cross-linker (genipin) to enhance its mechanical properties and improve its resistance to enzymatic degradation. In vitro testing results demonstrated that the stiffness of the genipin cross-linked PADM was improved and biodegradation rate was decreased. Results of cell proliferation assays showed that the cross-linking reaction by genipin did not undermine the cytocompatibility of PADM. Furthermore, genipin cross-linking imparted an observable fluorescence allowing visualization of the scaffold's three-dimensional (3D) porous structure and cell distribution by confocal laser scanning microscopy (CLSM). Immunostaining of the cell nuclei and cytoskeleton indicated that MC3T3-E1 preosteoblasts were tightly adhered to and uniformly distributed onto the cross-linked PADM scaffold. Results of this study suggest that the 3D porous genipin cross-linked PADM with intrinsic fluorescence may have broader applications for tissue engineering scaffolds where higher mechanical stiffness is needed.

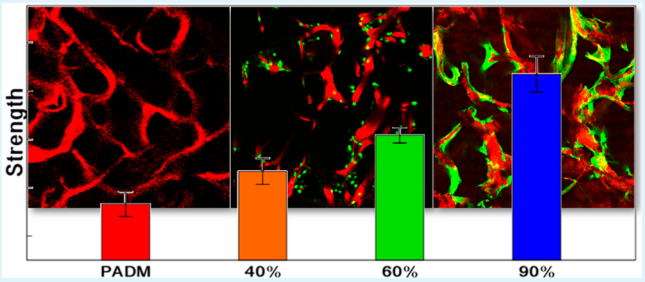

KEYWORDS: *porcine acellular dermal matrix, genipin, cross-link, fluorescence, biocompatibility, tissue engineering scaffold*

1. INTRODUCTION

Tissue engineering has aimed to repair and regenerate a variety of defect tissues and organs through combination of cells, scaffolds, and biomolecules since it first appeared in the 1980s.[1−3] Scaffolds not only serve as a support for cells but also provide a biochemical and physical environment similar to native tissue, which plays an import role in promoting cell adhesion, proliferation, differentiation, and tissue neogenesis.[3−5] Scaffolds need to be porous to allow for cells to distribute throughout and allow for efficient mass transport of nutrients, oxygen, growth factors, and waste products while enough stiffness to withstand the surrounding mechanical stresses during tissue neogenesis is also required.[3,6,7] Good biocompatibility and appropriate degradation rate consistent with the formation of new tissue are also necessary for tissue engineering scaffolds.[8] The in vivo extracellular matrix (ECM) provides a number of cues including topography, mechanical properties, and immobilized growth factors which directly regulate essential cellular functions such as morphogenesis, differentiation, proliferation, adhesion, and migration.[9,10] Considering these factors, many researches focus on designing and preparing three-dimensional (3D) porous scaffolds with good biocompatibility and bioactivity that mimic native ECM.[11−13]

As a kind of natural ECM, porcine acellular dermal matrix (PADM) is derived from porcine skin by removing cells and cellular components, leaving the native structure of the dermal meshwork only. It has drawn the extensive attention of researchers due to its good biocompatibility, bioactivity, biodegradability, and porous structure.[14−16] PADM, mainly composed of type I and II collagen, has a similar structure and immunogenicity to human acellular dermal matrix[17] and has been successfully used in covering full thickness burn wounds in clinical practice.[16] In our previous work, a biocompatible 3D porous PADM (pore size is about 100−150 μm) was prepared by a low cost method.[18] When preparing acellular matrix, a

Received: October 9, 2012
Accepted: December 17, 2012
Published: December 17, 2012

concern with the decellularization processes is that the detergent interaction, enzyme digestion, and mechanical vibration may loosen the collagen fibrils and disrupt the microstructure of the ECM which will reduce the mechanical stiffness and accelerate the biodegradation rate of the decellularized matrix.[19−21] Thus, maintaining the mechanical properties and tuning the degradation rate of PADM are important in PADM-based scaffolds design.

Generally, cross-linking agents are used to improve the mechanical properties and slow down the biodegradation rate of collagen-based biomaterials.[22,23] A cross-linking reaction can be induced by UV light,[24] chemical reagents (like glutaraldehydes,[25] carbodiimide[26]), and enzyme catalysis (such as transglutaminase[27]). However, most of them are related to artificial synthesized collagen scaffolds. To the best of our knowledge, there are few works about cross-linkage of PADM to improve its mechanical properties and control the biodegradation rate.

As a low-cost and highly efficient chemical cross-linker, glutaraldehyde is commonly used as a reinforcing agent for collagen-based biomaterials.[25] However, the cytotoxic properties of glutaraldehyde limit the application of glutaraldehyde cross-linked biomaterials.[28] Recently, a natural nontoxic cross-linker, genipin (an aglycone of geniposide extracted from gardenia fruit), has been widely used in preparing collagen-based and chitosan-based biomaterial.[29−34] Genipin not only has the ability to enhance the strength of tissue engineering materials but also endows the materials with an intrinsic fluorescence, which has been investigated in fingerprint reagent detection and scaffold structure characterization.[35−37] Furthermore, the fluorescent properties of genipin cross-linked scaffolds can provide an effective way to image the cell-scaffold interface, trace cell adhesion, follow cell migration and proliferation, and investigate the scaffold degradation process with a confocal laser scanning microscope (CLSM).[38]

The aim of this report is to broaden the application of the collagen-based natural extracellular matrix PADM as a tissue engineering scaffold. We cross-linked PADM with genipin to controllably enhance its mechanical stiffness and reduce its biodegradation rate. Mechanical testing and in vitro degradation tests were performed to assess the effects of cross-linking. MC3T3-E1 mouse preosteoblasts were used to investigate the cytocompatibility of the cross-linked PADM. Taking advantage of its intrinsic fluorescence, we also characterized the cell-scaffold interaction, cell distribution and adhesion.

2. MATERIALS AND METHODS

2.1. Preparation of PADM. Porcine acellular dermal matrix (PADM) was prepared as described in our previous report.[18] Briefly, fresh porcine skin purchased from a local slaughter-house was completely cleaned to excise the subdermal fat tissue and the hairs. Then the skin was purified through alkaline treatment and enzyme and detergent extraction methods to remove the fat and cells. After washing carefully in distilled water, the moisture-laden porcine acellular skin was frozen at −80 °C and lyophilized at −60 °C for 4 h. The resulting PADM sheets were punched into disk-shaped samples 8 mm in diameter (Supporting Information Figure S1).

2.2. Cross-linking Processes. The PADM samples were cross-linked in aqueous genipin (Hu Yun Co. Ltd. Shanghai, China) solutions with different concentrations (0.025%, 0.05%, 0.1%, 0.25%, 0. 5%, and 1%) buffered with phosphate buffered saline (PBS, 0.1 M, pH = 7.4, Sigma) at 37 °C for 6 h. Then, the cross-linked PADM was washed in distilled water and lyophilized at −60 °C.

The cross-linking degree, defined as the percentage of primary amine groups in PADM reacted with genipin,[31] was determined by a ninhydrin assay.[39] Primary amine groups can react with ninhydrin solution, forming a purple colorimetric response whose absorbance at 570 mm can reflect primary amine group amount. PADM and the cross-linked PADM samples were immersed in a ninhydrin solution (170 mg ninhydrin and 30 mg hydrindantin dissolved in 20 mL ethylene glycol monomethyl ether) for 15 min in a boiling water bath. Then, the reacted ninhydrin solution was cooled to room temperature and diluted in 60% ethanol. Its absorbance at 570 nm was measured by a microplate reader (MULTISKAN MK3, Thermo, USA). The cross-linking degree was calculated by the following formula

$$\text{Cross-linking degree} = (1 - C/N) \times 100\%$$

where C and N indicate the absorbance values of ninhydrin solution after being reacted with cross-linked and noncross-linked PADM, respectively.

2.3. Scanning Electron Microscopy Observation. After the cross-linking reaction, the moisture-laden PADM samples were frozen at −80 °C and cut into small pieces at freezing state. The small pieces of samples were lyophilized at −60 °C for 4 h and then coated with gold for 55 s on a conductive tape using an ion sputter coater (E-1045, Hitachi, Japan). A scanning electron microscope (SEM, S-4800, Hitachi, Japan) was used to characterize the morphology of PADM and genipin cross-linked PADM at an accelerating voltage of 5 KV. The pore parameters were analyzed by measuring diameters and wall thicknesses of ten typical channels on SEM images. The thinnest part of the channel wall was considered to be its thickness.

2.4. Mechanical Testing. Before measuring the mechanical properties, the disk-shaped PADM samples (8 mm in diameter and 2 mm in thickness) were rinsed in PBS to ensure the sample was hydrated. The compressive properties of PADM and cross-linked PADM with different cross-linking degrees were measured on a computer-controlled WDW-1 universal material testing machine (Zhixing Co., China) with a cross head speed of 0.6 mm/min maintained until failure. The modulus was defined as the slope of a linear fit to the stress−strain curve over 2−5% strain.[40]

2.5. In vitro Degradation. All samples for degradation rate testing were cut into small bricks weighing about 15 mg each. The samples were first placed in 1.5 mL of 100 mg/mL collagenase Tris-HCl buffer solution (50 mM, pH = 7.4), then the solution was incubated at 37 °C with stirring for 1, 2, 3, and 4 days, respectively. The collagenase solution was replaced every 24 h. At the end of each time point, three samples for each group were removed from the solution, washed with distilled water, and then lyophilized. The biodegradation of PADM and genipin cross-linked PADM was evaluated with the degradation percentage calculated from the mass of residual PADM samples after enzymatic digestion.

2.6. Fluorescence Study of Genipin Cross-linked PADM. The fluorescence of genipin cross-linked PADM was investigated by confocal laser scanning microscope (CLSM, Leica, Germany) and fluorescence spectrometer (FLS920, Edinburgh, UK). Samples were kept dry and pressed into thin slices under pressure of 100 KPa. Then, the sliced samples were separately excited by 488 and 633 nm excitation using a fluorescence spectrometer to measure their fluorescence emission spectra. Samples rinsed in PBS were used to take fluorescent images by CLSM at the excitation wavelength of 633 nm.

2.7. Cell Culture. MC3T3-E1 mouse preosteoblast cells (Cell Bank of Chinese Academy of Sciences) were selected as a model to evaluate the biocompatibility of genipin cross-linked PADM in vitro. PADM and genipin cross-linked PADM samples were first sterilized in 75% ethanol for 12 h, washed three times in sterile distilled water and sterile PBS in sequence, and then immersed in α-minimum essential medium (α-MEM, Gibco) overnight to avoid cellular nutrient depravation resulting from adsorption by PADM.[18] Finally, scaffolds were seeded with 400 μL cell suspension containing 2000 cells in 48-well-plates. Cells were cultured with α-MEM medium supplemented with 10% fetal bovine serum (FBS, Gibco) and 1% penicillin−

streptomycin in a humidified atmosphere of 5% CO_2 at 37 °C. Culture medium was replaced every 48 h.

2.8. Cell Proliferation. A Cell Count Kit-8 (CCK-8, Dojindo Molecular Technology, Gaithersburg, MD) was used to quantitatively evaluate cell viability on various samples after cultivation for 1, 3, and 5 days. Each tested sample was taken out to a new 48-well plate containing 400 μL α-MEM medium and 40 μL CCK-8, followed by incubation at 37 °C for 3 h. Then, solution (200 μL) was taken from each well and transferred to a well of a 96-well plate to measure the absorbance at 450 nm by a microplate reader (MULTISKAN MK3, Thermo, USA).

2.9. Cell Distribution, Adhesion, and Cytoskeleton Organization. The cell distribution, adhesion, and morphology on genipin cross-linked samples stained with nucleic acid dye, acridine orange (AO, Invitrogen), and Alexa Fluor 488 phalloidin (Invitrogen) were examined using CLSM at day 2 and 5. Briefly, for staining nuclei, the cell-loaded samples were fixed with 4% paraformaldehyde for 1 min, and then stained in 0.01% acridine orange solution for 1 min. For immunofluorescence measurements of F-actin, the cell-loaded samples were fixed with 3.7% formaldehyde solution for 10 min, then permeabilized with 0.1% Triton X-100 (Sigma) for 5 min and blocked with PBS containing 1% bovine serum albumin (BSA, Sigma) for 30 min. The samples were then stained with phalloidin conjugated to Alexa Fluor 488. And finally, all samples were examined at excitation wavelengths of 488 and 633 nm.

2.10. Statistics Analysis. The statistical analysis of all the experimental data was performed using SPSS version 17.0 (SPSS Inc., Chicago, Illinois). Data were reported as means ± standard deviation. Statistical comparisons between groups were performed by Mann–Whitney U test, and a Kruskal–Wallis test was used to compare the results among multiple groups. Statistical significance was accepted at $p \leq 0.05$.

3. RESULTS AND DISCUSSION

3.1. Cross-linking Degree. Figure 1 shows the evolution of the cross-linking degree (the cross-linked primary amine group percentage of total primary amine group) of genipin cross-linked PADM at different concentrations after 6 h of reaction determined by ninhydrin assay. The cross-linking degree increases significantly with the increase of genipin concentration below 0.25%. When genipin concentration reaches 0.5%, the cross-linking degree approaches a maximum and plateau, implying 0.5% is the saturated genipin concentration for cross-linking PADM.

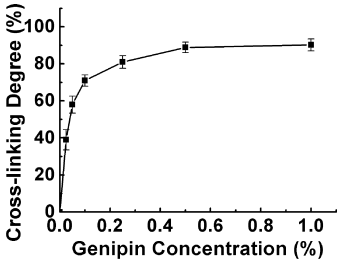

Figure 1. Cross-linking degree of PADM cross-linked by genipin at different concentrations after 6 h of reaction. The error bar designates standard deviation obtained from three parallel samples.

To investigate the effect of cross-linking degree on mechanical properties, biodegradation ability, and cytocompatibility of PADM, samples with cross-linking degree of approximately 40% (cross-linked in 0.025% genipin solution), 60% (cross-linked in 0.05% genipin solution), and 90% (cross-linked in 0.5% genipin solution) were prepared. PADM samples without cross-linking were used as control.

3.2. SEM Observation. As Figure 2a and b show, PADM before cross-linking has a 3D porous structure. The mean value of pore parameters was analyzed by measuring diameters and wall thicknesses of ten typical channels. The diameter and wall thickness of the interconnected channels are 98 ± 30 and 9 ± 3 μm, respectively. Figure 2c shows the surface topology of the channel wall. It illustrates the intertwined collagen fibrils within the channel walls. Each fibril has periodic striations (insert) formed by the staggering of the tropocollagen. The interconnection between collagen fibrils is loose due to the disruption during the decellularization processes. Compared to uncross-linked PADM, genipin cross-linked PADM retains a similar 3D porous microstructure (Figure 2d and e). No obvious variation of the morphology, including channel size (105 ± 28 μm) and the wall thickness (10 ± 2 μm) of the porous PADM scaffold is observed. The 3D porous structure of PADM and cross-linked PADM is favorable to cell perfusion into the interior of the scaffold. Figure 2f illustrates the collagen fibrils aligned and tightly connected, probably due to the cross-linking by genipin. These results show that the genipin cross-linking reaction does not alter the 3D porous structure of PADM but improves the interconnection among collagen fibrils.

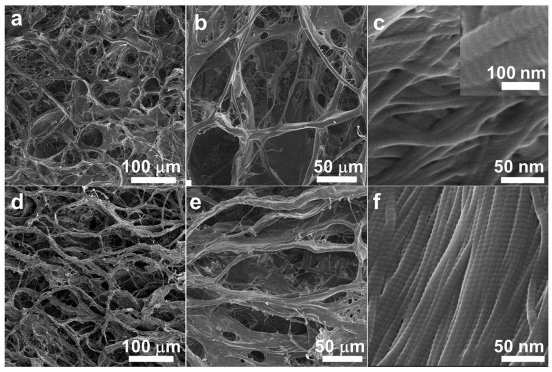

Figure 2. SEM images of PADM (a–c) and genipin cross-linked PADM (cross-linking degree is 90%) (d–f). (a and d) Interconnected porous structure. (b and e) Structure of typical channels. (c and f) Morphology of channel wall.

3.3. Mechanical Properties. Generally, the compressive elastic modulus (CEM) is used to evaluate the mechanical properties of bone scaffolds.[41,42] Figure 3 shows the CEMs of PADM samples with different cross-linking degrees under wet conditions. The CEMs of different samples increase significantly with the increase of cross-linking degree (*$p \leq 0.05$, #$p \leq 0.05$). The CEM of PADM with a cross-linking degree about 90% is 385 ± 21 KPa, which is three times higher than that of uncross-linked PADM (116 ± 14 KPa). This result indicates that cross-linking by genipin improves the stiffness of PADM under wet conditions. Additionally, the mechanical properties can be tuned via tuning the cross-linking degree by varying the genipin concentration. The initial stiffness of scaffold transplanted into the defect site plays an important role in supporting and resisting against the surrounding pressures. Previously, it was shown that cross-linking and the resulting increase in mechanical stiffness could enhance the cellular activity within collagen-based artificial porous scaffold.[43] Additionally, the improved stiffness may facilitate scaffold integration with surrounding native tissues and decrease the

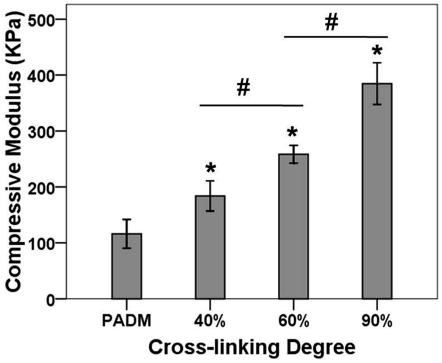

Figure 3. Compressive elastic modulus of PADM and PADM scaffolds at various cross-linking degrees under wet conditions. Statistical significance was evaluated via Mann–Whitney U test. * indicates statistical significance relative to PADM ($p \leq 0.05$); # indicates statistical significance between designated groups ($p \leq 0.05$). Three parallel samples were used.

rate of implant failure.[2] These results highlight the application potential for genipin cross-linked PADM in tissue engineering.

3.4. In vitro Biodegradation. Enzymatic digestion with collagenase is often used to investigate biodegradation of collagen-based scaffolds in vitro.[29,31,44] Degradation percentages of samples with varying cross-linking degrees as a function of enzymatic digestion time are shown in Figure 4. All samples

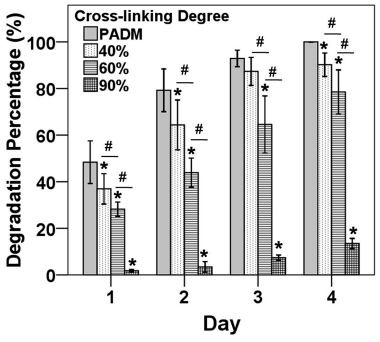

Figure 4. Degradation percentages of PADM and PADM scaffolds at various cross-linking degrees after 1, 2, 3, and 4 days enzymatic treatment. Statistical significance was evaluated via Mann–Whitney U test. * indicates statistical significance relative to PADM at same time point ($p \leq 0.05$); # indicates statistical significance between designated groups ($p \leq 0.05$). Three parallel samples were used.

are biodegraded after long time treatment with enzyme. However, at every time point, the degradation percentages of different samples significantly decrease with the increase of cross-linking degree (*$p \leq 0.05$, #$p \leq 0.05$). After four days of treatment, the uncross-linked PADM is completely degraded while the degradation percentage of PADM samples with a cross-linking degree of 90% is less than 15%. This result suggests that degradation rate of PADM can be controlled by tuning the cross-linking degree with varying concentrations of genipin.

In tissue engineering, as new functional tissue forms, scaffolds should ideally be degraded with a degradation rate that can match the speed of tissue regeneration.[3] Genipin cross-linked PADM has the advantageous property of tunable degradation rate controlled by the cross-linking degree.

3.5. Scaffold Fluorescence. As we reported previously,[18] chitosan scaffolds become fluorescent after cross-linking with genipin. To determine if genipin cross-linking can induce fluorescence in PADM, the fluorescent emission spectra of samples with 90% cross-linking were measured. The fluorescence emission spectra in Figure 5A show that three

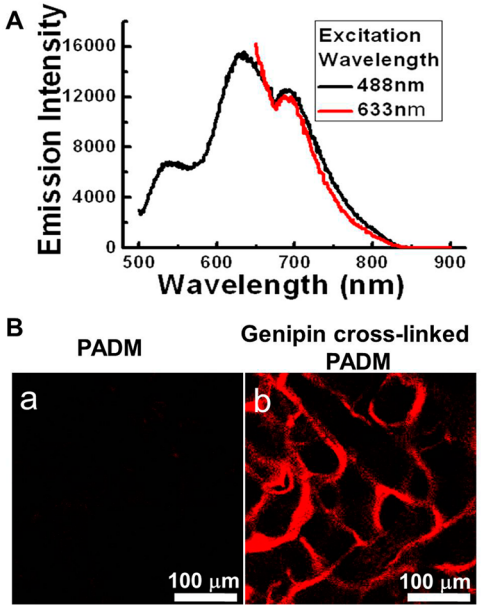

Figure 5. Fluorescence of genipin cross-linked PADM. (A) Fluorescence emission spectra of genipin cross-linked PADM (cross-linking degree is 90%) at the excitation wavelength of 488 and 633 nm. (B) Confocal laser scanning micrographs of uncross-linked PADM (a) and genipin cross-linked PADM (b) when excited at the wavelength of 633 nm.

broad fluorescence emission peaks occur at 520, 630 and 690 nm with 488 nm light excitation. The peaks at 630 and 690 nm overlap. When the sample is excited at 633 nm, only one broad fluorescence emission peak at 690 nm is observed within the region from 650 to 900 nm. As the confocal laser scanning micrographs in Figure 5B, an excitation with 633 nm results in the red fluorescence of the scaffold while no fluorescence is observed for uncross-linked PADM. The pore sizes determined from the fluorescent images are consistent with SEM results.

Genipin is a special cross-linking agent. After cross-linking with genipin, many polymers obtained fluorescent properties. Sundararaghavan et al.[45] prepared fluorescent collagen–genipin gel and studied the relationship between mechanical properties and fluorescence. In another study, taking advantage of the genipin caused fluorescence, Chen et al.[36] studied the properties of genipin cross-linked alginate–chitosan microcapsules by CLSM. Genipin has been found to cross-link polymers through nucleophilic attack by primary amine group on the C_3 atom of genipin, subsequently embedding a tertiary nitrogen in the six-membered ring in place of an oxygen atom.[45,46] The π–π^* conjugation formed by this reaction can be used to explain the fluorescent characteristics[35,47] So the fluorescent properties of cross-linked PADM are attributed to the reaction between genipin and the primary amine groups in collagen-based PADM. The intrinsic fluorescence endowed by genipin cross-linking suggests a promising application for imaging to track scaffold degradation.[38]

3.6. Cell Proliferation. MC3T3-E1 preosteoblasts have been extensively used for assessing the biocompatibility of bone scaffolds.[48,49] As shown in Figure 6, the result of a CCK-8 assay

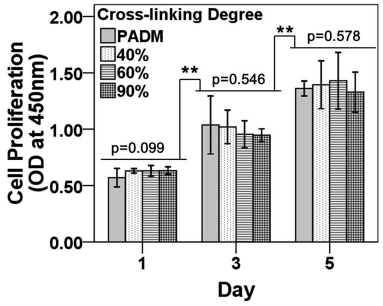

Figure 6. Proliferation of MC3T3-E1 preosteoblasts on PADM and different cross-linking degree PADM scaffolds after 1, 3, and 5 days. Statistical significance was evaluated via Mann–Whitney U test between groups and Kruskal–Wallis test for multiple groups. ** indicates statistical significance between designated groups ($p \leq 0.01$). Three parallel samples were used.

clearly demonstrates that MC3T3-E1 preosteoblast cells proliferate well and exhibit a good growth state on uncross-linked and cross-linked PADM samples (**$p \leq 0.01$). And at all time points considered there is no significant difference between the cells on cross-linked and uncross-linked PADM, which suggests that the cross-linking reaction has no influence on the biocompatibility of PADM. Genipin itself has no toxicity,[29] and during cross-linking processes, genipin reacts with primary amine groups in collagen-based materials and does not form any other byproducts besides H_2O,[45,46] which can explain why the cross-linking reaction has no influence on the biocompatibility of PADM and genipin cross-linked PADM has good biocompatibility.

3.7. Cell Distribution on Genipin Cross-linked PADM.

The CLSM images of the distribution and localization of MC3T3-E1 preosteoblasts at different days cultured on genipin cross-linked PADM with 90% cross-linking degree are shown in Figure 7. Figure 7a and d show the nuclei of cultured cells imaged with 488 nm excitation. Figure 7b and e show the genipin cross-linked PADM scaffolds imaged with 633 nm excitation. Figure 7c and f are the overlays of these two images and demonstrate that the location of the cell nuclei coincides with the scaffold. This indicates that cells mainly distributed on

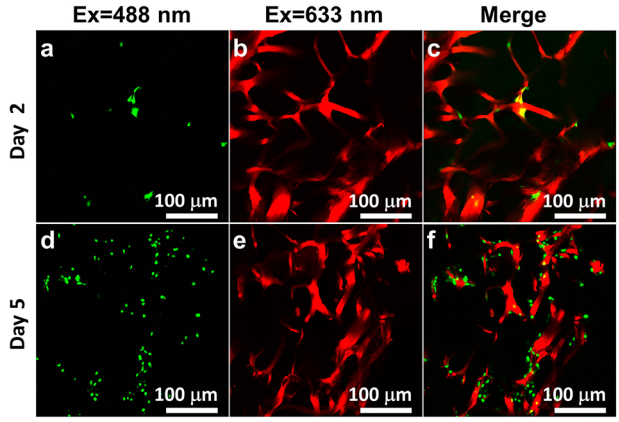

Figure 7. CLSM images of the distribution of MC3T3-E1 preosteoblasts stained with Acridine Orange on genipin cross-linked PADM (cross-linking degree is 90%) at different days excited at the wavelength of 488 (a and d) and 633 nm (b and e). Images c and f are the overlays of a, b and d, e respectively. The bright green regions are nuclei, and the red regions are the PADM.

the channel wall of genipin cross-linked PADM. Compared to day 2 (Figure 7a–c), cell density at day 5 (Figure 7d–f) increases apparently, which is consistent with cell proliferation result. And as cell density increases, cells distributed on the channel wall more uniformly.

3.8. Cell Adhesion and Morphology.

The intrinsic fluorescence of the genipin cross-linked PADM provides an effective way to image the cell–scaffold interaction and monitor cell adhesion, localization, and migration on the surface of the PADM. Figure 8 shows the CLSM images of MC3T3-E1

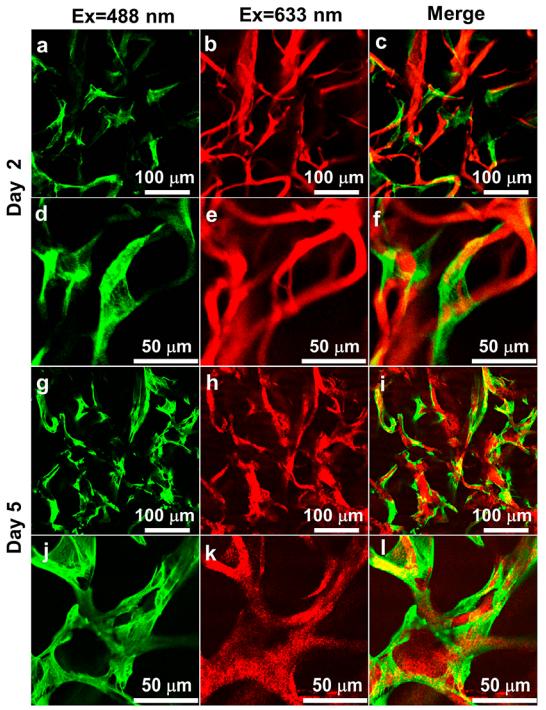

Figure 8. CLSM images of MC3T3-E1 preosteoblasts stained with Alexa Fluor 488 Phalloidin on genipin cross-linked PADM (cross-linking degree is 90%) at different days excited at the wavelength of 488 (a, d, g, and j) and 633 nm (b, e, h, and k). Images c, f, i, and l are the overlays of a, b; d, e; g, h; and j, k, respectively. The bright green regions are the cytoskeleton, and the red regions are the PADM.

preosteoblasts cultured on genipin cross-linked PADM (cross-linking degree is 90%) at different days excited at the wavelengths of 488 and 633 nm after staining with Alexa Fluor 488 Phalloidin. Figure 8a, d, g, and j show the morphology of the stained cells on the sample, and Figure 8b, e, h, and k show the morphology of genipin cross-linked PADM scaffold. As shown in Figure 8c and f, after 2 days of culture on genipin cross-linked PADM, MC3T3-E1 preosteoblasts stained with Alexa Fluor 488 Phalloidin (bright green regions) are adhered tightly onto the cross-linked PADM surface (red regions) and retain their initial morphology. Compared to day 2, cell density at day 5 is higher on genipin cross-linked PADM and cells adhered more tightly onto the channel surface (Figure 8i and l).Channel walls are nearly fully covered with cells (the dark regions without cells are channels). These results combined with the cells distribution results indicate that the genipin cross-linked PADM facilitates MC3T3-E1 preosteoblasts adhesion and proliferation, and cells on scaffold have a good growth state. Cells distribution and adhesion properties can be easily obtained by CLSM using

dx.doi.org/10.1021/am302272k | ACS Appl. Mater. Interfaces 2013, 5, 344–350

the fluorescent properties of the genipin cross-linked PADM. The fluorescent properties may facilitate getting more detailed information of cell−scaffold interaction in tissue engineering during tissue formation.

We previous incorporated a hydroxyapatite nanostructure into PADM by biomimetic mineralization and studied its potential application as bone scaffold.[18] The inorganic hydroxyapatite is good reinforcing agent, and the compressive elastic modulus of hydroxyapatite−PADM composite approached at nearly 600 KPa under wet conditions. The biodegradation rate of hydroxyapatite−PADM composite decreased apparently compared with pure PADM. However, compared to a long biomimetic mineralization period (15 days), in this work, only a 6 h reaction with genipin could significantly improve the mechanical properties of PADM. Moreover, the mechanical properties and biodegradation rate were more easily controlled by tuning the genipin concentration. The genipin reinforced PADM can be a basic scaffold for different tissue engineering application occasions, such as, skin, blood vessel, nerve, etc. Of course, it can be used for bone tissue engineering scaffold by assembling a layer of hydroxyapatite nanostructures through a biomimetic mineralization process. Because the mechanical properties of genipin cross-linked PADM are much higher than those of uncross-linked PADM, the composite of genipin cross-linked PADM and hydroxyapatite should be stronger than the hydroxyapatite−PADM scaffold prepared in our previous study. The related work is ongoing in our group.

As a natural nontoxic cross-linker, genipin has been widely used in stabilizing decellularized matrix.[29,31,32] Bottino et al.[50] have investigated the effect of cross-linkers, including genipin and glutaraldehyde, on tensile strength and elastic modulus of human acellular dermal matrix (HADM) systemically, concluding that all the cross-linkers including genipin can reinforce the HADM effectively. However, they did not notice the fluorescent properties and have not assessed the cytocompatibility of the cross-linked HADM. In this work, we focus on tuning the genipin cross-linking effect of PADM on its mechanical properties and biodegradation rate and demonstrated its practicability. Furthermore, we assessed the cytocompatibility of genipin-linked PADM using MC3T3-E1 preosteoblasts and proved genipin is safe for the cell culture, which is very important for the application of such reinforced scaffold. Moreover, we put more attention on the fluorescent properties of genipin cross-linked PADM, demonstrating that it is convenient to investigate cell distribution, adhesion, and other cell−scaffold interactions during culturing cells on genipin cross-linked PADM scaffold by CLSM without adding any other fluorescent substances.

The intrinsic fluorescence of genipin cross-linked PADM may be further used in evaluating its degradation processes without injury in vivo. As the fluorescence of genipin cross-linked materials is caused by the reaction between genipin and primary amine groups in materials,[35,47] genipin may endow other primary amine groups contained materials fluorescence, and it is helpful to characterize the materials with fluorescence microscopy. And genipin could be used in other areas where enhanced mechanical properties or fluorescence is need

4. CONCLUSION

The nontoxic cross-linking agent, genipin, was successfully used to cross-link 3D porous natural porcine acellular dermal matrix (PADM). Cross-linking treatment enhances the mechanical stiffness of the scaffold and reduces the rate of degradation. These properties can be tuned by varying the cross-linking degree through changes the concentration of genipin solution. Culturing MC3T3-E1 preosteoblasts on the cross-linked PADM scaffolds demonstrated that cells could adhere, proliferate, and spread onto the channel surface of cross-linked PADM. Additionally, cross-linking with genipin endows PADM with fluorescence that enables observation and characterization of the cell-scaffold interaction, cell distribution and adhesion. These results indicate the potential applications of genipin cross-linked PADM scaffolds in tissue engineering and regeneration.

■ ASSOCIATED CONTENT

Ⓢ Supporting Information

Digital photos of PADM and genipin cross-linked PADM samples. This material is available free of charge via the Internet at http://pubs.acs.org.

■ AUTHOR INFORMATION

Corresponding Author

*E-mail: hongliu@sdu.edu.cn (H.L.). Tel.: (+86) 531-88362807. Fax: (+86) 531-88362807. E-mail: imwangyj@scut.edu.cn (Y.W.).

Notes

The authors declare no competing financial interest.

■ ACKNOWLEDGMENTS

This research was supported by NSFC (NSFDYS: 50925205, 51102152, 51002089, 81102229, IRG: 51021062), National Basic Research Program of China (Grant No. 2012CB619100) and the National and the Program of Introducing Talents of Discipline to Universities in China (111 program No. b06015), the Natural Science Funds for Distinguished Young Scholar of Shandong Province (JQ201117), the Independent Innovation Foundation of Shandong University (2010JQ004, 2012GN006), and China Postdoctoral Science Foundation (10000071311003).

■ REFERENCES

(1) Vacant, R.; Vacanti, J. P. *Science* **1993**, *260*, 920−926.
(2) Rose, F. R.; Oreffo, R. O. *Biochem. Biophys. Res. Commun.* **2002**, *292*, 1−7.
(3) Griffith, L. G.; Naughton, G. *Science* **2002**, *295*, 1009−1014.
(4) Hollister, S. J. *Nat. Mater.* **2005**, *4*, 518−524.
(5) Holzwarth, J. M.; Ma, P. X. *Biomaterials* **2011**, *32*, 9622−9629.
(6) Freed, L. E.; Guilak, F.; Guo, X. E.; Gray, M. L.; Tranquillo, R.; Holmes, J. W.; Radisic, M.; Sefton, M. V.; Kaplan, D.; Vunjak-Novakovic, G. *Tissue Eng.* **2006**, *12*, 3285−3305.
(7) Ma, P. X. *Mater. Today* **2004**, *7*, 30−40.
(8) Szpalski, C.; Wetterau, M.; Barr, J.; Warren, S. M. *Tissue Eng., Part B* **2012**, *18*, 246−257.
(9) Tsang, K. Y.; Cheung, M. C.; Chan, D.; Cheah, K. S. *Cell Tissue Res.* **2010**, *339*, 93−110.
(10) Hynes, R. O. *Science* **2009**, *326*, 1216−1219.
(11) Dvir, T.; Timko, B. P.; Kohane, D. S.; Langer, R. *Nat. Nanotechnol.* **2011**, *6*, 13−22.
(12) Stevens, M. M.; George, J. H. *Science* **2005**, *310*, 1135−1138.
(13) Ma, P. X. *Adv. Drug Delivery Rev.* **2008**, *60*, 184−198.
(14) Srivastava, A.; DeSagun, E. Z.; Jennings, L. J.; Sethi, S.; Phuangsab, A.; Hanumadass, M.; Reyes, H. M.; Walter, R. J. *Ann. Surg.* **2001**, *233*, 400.
(15) Chai, J. K.; Liang, L. M.; Yang, H. M.; Feng, R.; Yin, H. N.; Li, F. Y.; Sheng, Z. Y. *Burns* **2007**, *33*, 719−725.

(16) Chai, J. K.; Liu, Q.; Feng, R. *Med. J. Chin. PLA* **2004**, *29*, 714−721.
(17) Ge, L. P.; Zheng, S. Q.; Wei, H. *Burns* **2009**, *35*, 46−50.
(18) Zhao, H.; Wang, G.; Hu, S.; Cui, J.; Ren, N.; Liu, D.; Liu, H.; Cao, C.; Wang, J.; Wang, Z. *Tissue Eng., Part A* **2011**, *17*, 765−76.
(19) Gorschewsky, O.; Puetz, A.; Riechert, K.; Klakow, A.; Becker, R. *Bio-Med. Mater. Eng.* **2005**, *15*, 403−411.
(20) Ott, H. C.; Clippinger, B.; Conrad, C.; Schuetz, C.; Pomerantseva, I.; Ikonomou, L.; Kotton, D.; Vacanti, J. P. *Nat. Med* **2010**, *16*, 927−933.
(21) Kasimir, M.; Rieder, E.; Seebacher, G.; Silberhumer, G.; Wolner, E.; Weigel, G.; Simon, P. *Nat. Med.* **2003**, *26*, 421−427.
(22) Zeeman, R.; Dijkstra, P. J.; van Wachem, P. B.; van Luyn, M. J.; Hendriks, M.; Cahalan, P. T.; Feijen, J. B. *Biomaterials* **1999**, *20*, 921−931.
(23) Rault, I.; Frei, V.; Herbage, D.; Abdul-Marak, N.; Hue, A. *J. Mater. Sci.: Mater. Med.* **1996**, *7*, 215−221.
(24) Weadock, K. S.; Miller, E. J.; Bellincampi, L. D.; Zawadsky, J. P.; Dunn, M. G. *J. Biomed. Mater. Res.* **1995**, *29*, 1373−1379.
(25) Olde Damink, L.; Dijkstra, P.; Luyn, M. J. A.; Wachem, P. B.; Nieuwenhuis, P.; Feijen, J. *J. Mater. Sci.: Mater. Med.* **1995**, *6*, 460−472.
(26) Powell, H. M.; Boyce, S. T. *Biomaterials* **2006**, *27*, 5821−5827.
(27) Chen, R. N.; Ho, H. O.; Sheu, M. T. *Biomaterials* **2005**, *26*, 4229−4235.
(28) Nimni, M. E. Bio-prosthesis Derived from Cross-linked and Chemically Modified Collagenous Tissues. In *Collagen*; Nimni, M. E., Cheung, D., Strates, B.; Kodama, M., Sheikh, K., Eds.; CRC Press: Boca Raton, FL, 1998; Vol *III*, p 1−38.
(29) Sung, H. W.; Huang, R. N.; Huang, L. L. H.; Tsai, C. C.; Chiu, C. T *J. Biomed. Mater. Res.* **1998**, *42*, 560−567.
(30) Chen, S. C.; Wu, Y. C.; Mi, F. L.; Lin, Y. H.; Yu, L. C.; Sung, H. W. *J. Controlled Release* **2004**, *96*, 285−300.
(31) Liang, H. C.; Chang, Y.; Hsu, C. K.; Lee, M. H.; Sung, H. W. *Biomaterials* **2004**, *25*, 3541−3552.
(32) Chang, Y.; Tsai, C. C.; Liang, H. C.; Sung, H. W. *Biomaterials* **2002**, *23*, 2447−2457.
(33) Chaubaroux, C.; Vrana, E.; Debry, C.; Schaaf, P.; Senger, B.; Voegel, J. C.; Haikel, Y.; Ringwald, C.; Hemmerlé, J.; Lavalle, P. *Biomacromolecules* **2012**, *13*, 2128−2135.
(34) Haag, J.; Baiguera, S.; Jungebluth, P.; Barale, D.; Del Gaudio, C.; Castiglione, F.; Bianco, A.; Comin, C. E.; Ribatti, D.; Macchiarini, P. *Biomaterials* **2012**, *33*, 780−789.
(35) Hwang, Y. J.; Larsen, J.; Krasieva, T. B.; Lyubovitsky, J. G. *ACS Appl. Mater. Interfaces* **2011**, *3*, 2579−2584.
(36) Chen, H.; Ouyang, W.; Lawuyi, B.; Prakash, S. *Biomacromolecules* **2006**, *7*, 2091−2098.
(37) Levinton-Shamuilov, G.; Cohen, Y.; Azoury, M.; Chaikovsky, A.; Almog, J. *J. Forensic Sci.* **2005**, *50*, 1367−1371.
(38) Wang, G.; Zheng, L.; Zhao, H.; Miao, J.; Sun, C.; Liu, H.; Huang, Z.; Yu, X.; Wang, J.; Tao, X. *ACS Appl. Mater. Interfaces* **2011**, *3*, 1692−1701.
(39) Moore, S.; Stein, W. H. *J. Biol. Chem.* **1954**, *211*, 907−913.
(40) Tierney, C. M.; Haugh, M. G.; Liedl, J.; Mulcahy, F.; Hayes, B.; O'Brien, F. J. *J. Mech. Behav. Biomed. Mater.* **2009**, *2*, 202−209.
(41) Nukavarapu, S. P.; Kumbar, S. G.; Brown, J. L.; Krogman, N. R.; Weikel, A. L.; Hindenlang, M. D.; Nair, L. S.; Allcock, H. R.; Laurencin, C. T. *Biomacromolecules* **2008**, *9*, 1818−1825.
(42) Lee, K. W.; Wang, S. F.; Yaszemski, M. J.; Lu, L. C. *Biomaterials* **2008**, *29*, 2839−2848.
(43) Haugh, M. G.; Murphy, C. M.; McKiernan, R. C.; Altenbuchner, C.; O'Brien, F. J. *Tissue Eng., Part A* **2011**, *17*, 1201−1208.
(44) Ma, L.; Gao, C.; Mao, Z.; Zhou, J.; Shen, J. *Biomaterials* **2004**, *25*, 2997−3004.
(45) Sundararaghavan, H. G.; Monteiro, G. A.; Lapin, N. A.; Chabal, Y. J.; Miksan, J. R.; Shreiber, D. I. *J. Biomed. Mater. Res., Part A* **2008**, *87*, 308−320.
(46) Englert, C.; Blunk, T.; Müller, R.; von Glasser, S. S.; Baumer, J.; Fierlbeck, J.; Heid, I. M.; Nerlich, M.; Hammer, J. *Arthritis Res. Ther.* **2007**, *9*, R47.
(47) Chen, H. M.; Wei, O. Y.; Bisi, L. Y.; Martoni, C.; Prakash, S. *J. Biomed. Mater. Res.* **2005**, *75A*, 917−927.
(48) Jackson, R. A.; Murali, S.; Van Wijnen, A. J.; Stein, G. S.; Nurcombe, V.; Cool, S. M. *J. Cell. Physiol.* **2007**, *210*, 38−50.
(49) Kong, H. J.; Boontheekul, T.; Mooney, D. J. *Proc. Natl. Acad. Sci. U. S. A.* **2006**, *103*, 18534−18539.
(50) Bottino, M. C.; Thomas, V.; Jose, M. V.; Dean, D. R.; Janowski, G. M. J. *Biomed. Mater. Res., Part B* **2010**, *95*, 276−282.